Robust Self-Healing Adhesives Based on Dynamic Urethane Exchange Reactions

Lillian M. Felsenthal, Subeen Kim, and William R. Dichtel*

Department of Chemistry, Northwestern University, 2145 Sheridan Road, Evanston, IL, 60208 USA

Abstract

Thermoset polyurethanes (PUs) have been successfully reprocessed as covalent adaptable networks (CANs) by catalyzing carbamate exchange. Here we extend bond exchange beyond the internal network crosslinks to create a dynamic urethane adhesive. Interfacing PU CANs to substrates with nucleophilic functional groups creates adhesives capable of reversible transcarbamoylation with the substrate, which has not been demonstrated previously by CAN adhesives. Two types of thermoset PU films were synthesized, one containing the green carbamate exchange catalyst $Zr(tmhd)_4$ and the other containing no catalyst. Although otherwise identical in chemical and network properties, as indicated by FT-IR spectroscopy and dynamic mechanical thermal analysis (DMTA), the film containing catalyst showed dynamic bond exchange behavior through stress relaxation analysis. When evaluated as an adhesive, the CAN film exhibited self-healing properties and retained its adhesive strength for five cycles, which is attributed to reversible covalent bonding to the glass substrate. This work expands industrially relevant CANs to structural adhesives and demonstrates their potential value in an application that presently employs PUs as single-use materials.

Keywords: covalent adaptable networks, polyurethane, transcarbamoylation, adhesive, urethane exchange, self-healing

Introduction

Structural adhesives play a crucial role in everyday life to bond joints in automotive, textile, construction, household, and other settings.[1-3] These adhesives require high strength and durability, and polymers such as urethane, acrylic, epoxy, phenolic, silicone are commonly employed.[3, 4] Polyurethanes (PUs) are highly tunable, allowing for specific properties to be matched for both industrial and household applications.[2, 5-10] Hot melt adhesives, comprised of thermoplastic polymers, provide ease of handling and reprocessability but lack the high tensile strength needed for structural bonding.[3, 11] Conversely, thermoset adhesives are typically cured directly on the adherends, providing enhanced strength.[1, 3] However, due to their crosslinked structure, recycling and reuse of thermoset adhesives are not possible.

Covalent adaptable networks (CANs) bridge this gap in reprocessing between thermoplastics and thermosets by employing dynamic crosslinks.[12-14] Under working conditions, the crosslinks are static, providing mechanical strength and durability to the network. When a stimulus is applied, usually heat, the crosslinks become dynamic, allowing for bond exchange to occur and imparting reprocessability to thermoset networks.[13, 14] Many dynamic chemistries have been employed in CANs, including thiourethanes, disulfides, boronic esters, Diels-Alder adducts, esters, imines, and siloxanes among many more.[9, 12, 13, 15-25] However, many of these CANs are designer networks that are not currently produced on industrial scales. Polyurethanes, on the other hand, are among the most produced polymers worldwide, with over 18 million tons being manufactured in 2019.[26, 27] Our group previously reported the ability to convert PU to CANs via the addition of a carbamate exchange catalyst.[28-30] We first used organotin compounds as carbamate exchange catalysts, which are bioaccumulative and toxic.[31] Recently, Sun and coworkers identified environmentally benign and non-toxic zirconium-based carbamate exchange catalysts that provide improved reprocessability to PU CANs without compromising their

mechanical properties.[32] In particular, zirconium tetrakis(2,2,6,6-tetramethyl-3,5-heptanedionate) [$Zr(tmhd)_4$] displayed rapid stress relaxation at loadings as low as 0.5 wt% zirconium. A more recent study by Kim *et al.* elucidated the mechanism of zirconium-based carbamate exchange catalysts and discovered that the zirconium complex catalyzes carbamate reversion to transiently generate Zr-bound isocyanates and alcohols to promote bond exchange in PU networks.[33]

Bond exchange in CANs is thought to occur between crosslinks within the network.[13] However, if a substrate is introduced with compatible surface functional groups, bond exchange will occur between the network and substrate. This provides enhanced adhesion through covalent bonding, as well as improved surface wettability.[16] The reversibility of the dynamic covalent bonds also impart self-healing properties to the adhesive and allow for traditional CANs reprocessing.[15, 16] While adhesive CANs have been demonstrated with a variety of linkages, including thiourethanes, disulfides, boronic esters, and oxime-carbamates, these are not currently used on industrial scales .[11, 15, 16, 18, 34] Herein, we demonstrate that PU CANs based on carbamate exchange have self-healing properties that allow for the retention of adhesive strength over multiple cycles through direct covalent bonding to the substrate. Moreover, these adhesives are industrially relevant and are synthesized from common PU monomers, polypropylene glycol and methylene diphenyl diisocyanate (MDI). Since the network crosslinks are dynamic, they can be reprocessed using compression molding with full recovery of chemical, network, and mechanical properties. This work extends beyond the traditional view of internal bond exchange in CANs, allowing for a clear path to industrially relevant applications.

Results and Discussion

To evaluate the impact of dynamic covalent bonds on mechanical and adhesive properties, two thermoset PU films were synthesized: one containing 1 mol% carbamate exchange catalyst, zirconium tetrakis(2,2,6,6-tetramethyl-3,5-heptanedionate) [$Zr(tmhd)_4$] (CAN film), and a control film containing no additional additives. Polypropylene glycol, a common polyol used in commercial PU adhesives, was chosen as the main hydroxyl-containing component in the network.[3] Hard segments of the network were comprised of MDI and a rigid polyester polyol (Figure 1). The polyester polyol provided additional rigidity, polarity, and hydrogen bond acceptors to increase the strength of the network (Figure S1). Since $Zr(tmhd)_4$ is both a carbamate exchange and gelling catalyst, no additional heat was needed to cure the network, while the control film containing no catalyst was heated at elevated temperature to promote polycondensation between isocyanate and hydroxyl groups. Both CAN and control film show complete conversion of the isocyanate monomer, as indicated by the lack of an N=C=O stretch in Fourier-transform infrared spectroscopy (FT-IR), which typically appears at 2285 cm^{-1} (Figure 2A). Gel fractions in dichloromethane upwards of 96% were obtained for both films, further confirming complete network formation (Table S1).

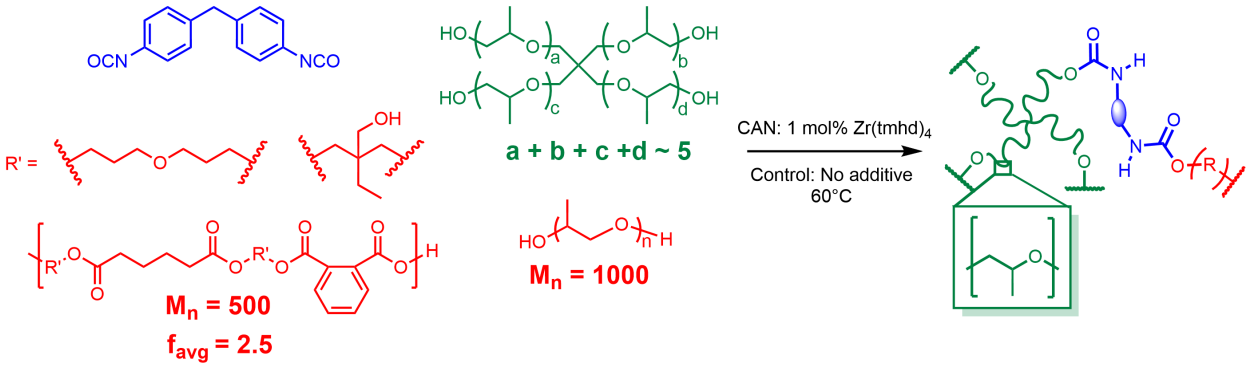

Figure 1. Synthesis of crosslinked PU films cured using heat (catalyst-free control film) or at room temperature in the presence of 1 mol% $Zr(tmhd)_4$ (CAN film).

Characterization of these films using FT-IR and dynamic mechanical thermal analysis (DMTA) show that the CAN and control film are chemically indistinguishable and have similar network properties. Both the CAN and control film were synthesized with 3 mol% excess isocyanate relative to hydroxyl groups. As a result, both networks display FT-IR stretches consistent with allophanate formation within the PU network (Figure 2B). The C=O stretch ranging from 1708-1725 cm^{-1} and the N-H deformation at 1513-1533 cm^{-1} are split peaks, indicating two separate carbonyl and urethane environments (Figure 2A). Additionally, an intense C-N stretch is seen at 1069 cm^{-1}. Combining the lack of a urea peak (typically seen around 1650 cm^{-1}) and the observed peak splitting, it can be concluded that excess isocyanates form allophanates within the PU network. Furthermore, DMTA of both films reveal a rubbery plateau in the storage modulus, indicating a crosslinked network (Figure 2C). Using Equation S1, the average molecular weight between crosslinks was calculated to be 782 g/mol for the CAN film and 525 g/mol for the control film (Table S1). Given that the smallest monomer between crosslinks has a molecular weight of 250 g/mol, the films have almost identical crosslink densities. A small peak can be seen in the tan (δ) curve for the CAN film just above 0°C (Figure 2C). Since only one T_g is seen using differential scanning calorimetry (Figure S2), the CAN film is homogenous and the small tan (δ) peak can be assigned as a beta transition rather than phase separation within the network. The presence of the bulky $Zr(tmhd)_4$ catalyst may contribute to localized backbone movements of the soft segments, resulting in a small beta transition.[35] Overall, spectral and thermomechanical characterization of the CAN and control film supports the conclusion that these films are identical in both chemical and network properties, therefore any performance differences between the two films can be directly attributed to the presence or absence of dynamic urethane bonds in the network.

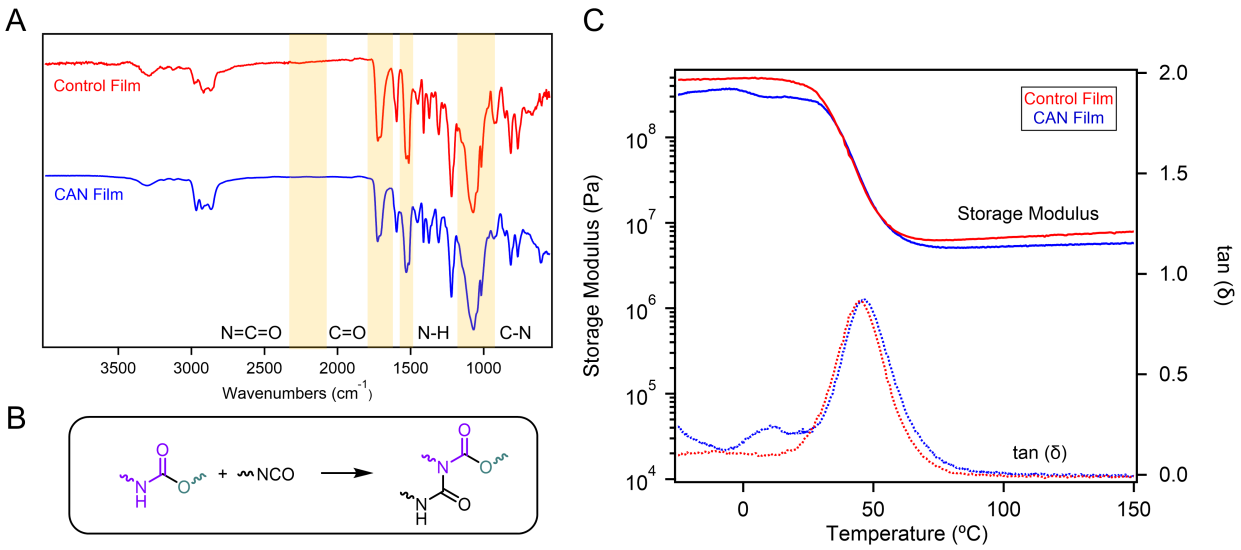

Figure 2. (A) FT-IR of catalyst-free control film and CAN film containing 1 mol% $Zr(tmhd)_4$. (B) Allophanate formation between carbamate and excess isocyanate. (C) DMTA of control film and CAN film.

The addition of $Zr(tmhd)_4$ in the CAN film creates dynamic urethane bonds that enable stress relaxation. Applying force to a dynamic network allows the bonds to undergo exchange reactions which relax the applied stress. Performing stress relaxation analysis (SRA) at typical reprocessing temperatures provides insight into the reprocessability of the dynamic network. When subjected to SRA at 160°C, the CAN film completely relaxes stress within 30 minutes, and the control film only partially relaxes stress under the same conditions (Figure 3A). Stress relaxation in the control film is attributed to a combination of hydrogen bonding dissociation, transallophanation, and urethane dissociation due to high temperature.[36] Since these processes occur at such long time scales, the urethane bonds in the control film can be treated as essentially static. The characteristic relaxation time, τ^*, is defined as the time at which the remaining stress is 1/e of the initial value. The CAN film had an average τ^* of 489 seconds at 160 °C (Table S2). Further analysis by applying a stretched exponential function fit (Equation S2) to the stress relaxation data afforded an average beta value of 0.85 (Table S2) with an average correlation

coefficient of 0.9995 (Figure 3A, Figure S3, Table S3). In this analysis, beta describes the distribution of relaxation events in the network, with a beta value of 1 corresponding to a single stress relaxation mechanism. In the CAN film there is one main mode of relaxation that can be attributed to urethane exchange. Deconvolution of a typical stress relaxation plot using a generalized Maxwell model produces a relaxation spectrum in which the characteristic time scale of each relaxation process is a local maximum (Figure 3B, Equation S3). For the CAN film, the global maximum occurs at 555 seconds (Figure 3B, Figure S4, Table S3), which is similar to the τ^* value of 489 seconds. This difference further confirms that dynamic behavior in the film is primarily associated with carbamate exchange, enabled by $Zr(tmhd)_4$. More minor relaxation processes appear at earlier time scales and are observed resulting from hydrogen bonding and transallophanation that may be present in the network (Figure 3B). Since urethane exchange is the clear mechanism of stress relaxation in the CAN film, we hypothesized that transcarbamoylation could occur with surface hydroxyl groups for reversible covalent bonding with a substrate.

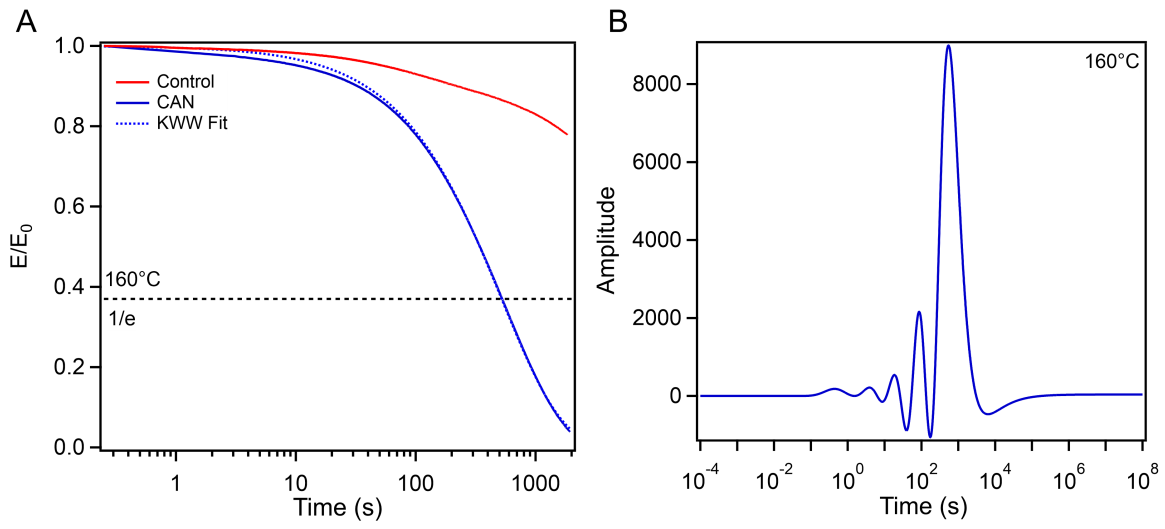

Figure 3. (A) Stress relaxation analysis of control and CAN films at 160°C. Dotted blue line indicates stretched exponential function fit to CAN film SRA. (B) Relaxation spectrum corresponding to CAN film at 160°C.

Lap shear testing demonstrated the self-healing ability of the CAN film compared to the control film and a commercial PU adhesive. Both the pre-synthesized CAN and control film were adhered to glass substrates by cutting the film to a specific size, then clamping and curing the joint at 150°C for two hours, allowing transcarbamoylation to occur between the films and surface hydroxyl groups on the glass. Employing thermogravimetric analysis (TGA), the CAN film was determined to be thermally stable under these curing conditions, indicated by an onset degradation temperature of 313°C and less than 4% mass loss when held at 150°C for 16 hours (Figure S5, Figure S6). The commercial PU adhesive was applied directly to wetted glass substrates and allowed to cure at room temperature, in accordance with product instructions. Initially, the CAN film and commercial PU adhesive performed similarly with an average lap shear strength around 1.5 MPa, while the control film had a significantly lower average lap shear strength 0.7 MPa (Figure 4). Since the films were post cured prior to lap shear sample preparation, all covalent bonding to the surface, and subsequently the lap shear strength, is a result of the reversible transcarbamoylation reaction. The control film does not contain catalyst that can accelerate transcarbamoylation, so there is likely to be little covalent bonding between the surface and the film, resulting in a lower average lap shear strength. Additionally, both the CAN and control film experienced adhesive failure, indicating that the weakest point in the lap shear sample occurred between the substrate and film. Therefore, the inherent strength of the adhesive films is larger than the measured lap shear strength. Conversely, the commercial PU adhesive experienced cohesive failure, meaning that the true network strength is accurately measured with lap shear testing. To heal the lap shear samples, the substrates and films were clamped together and heated at 150 °C for two hours. While the commercial PU adhesive showed no recovery of lap shear strength, the CAN film retained its adhesive strength over five healing cycles, demonstrating reversible covalent

bonding to the substrate through transcarbamoylation between surface hydroxyl groups and the CAN film (Figure 4). The control film recovered some of its adhesive properties through uncatalyzed bond exchange at the high curing temperature, however the control film did not recover any adhesive strength beyond the third healing cycle. In each healing cycle, the CAN film significantly outperformed both the control film and the commercial PU benchmark ($p < 0.1$ using a one-tailed T-test with unequal variance). The CAN film exhibited an average strength recovery ratio of 86% over the course of the experiment. After 5 healing cycles, the CAN film showed no chemical differences using FT-IR (Figure S7), indicating that a lack of available surface hydroxyl groups on the glass substrate may result in lower transcarbamoylation and consequently a lower lap shear strength. Furthermore, when the adhesive films were applied to silanized glass substrates, which lack surface hydroxyl groups, the lap shear strength was significantly lower than the untreated glass substrates (Figure S8). In contrast, after plasma treating the glass substrates to increase the number of surface hydroxyl groups, both the CAN and control films showed an increase in average lap shear strength (Figure S8). This confirms that dynamic covalent bonding of the CAN film to substrates occurs through transcarbamoylation with surface hydroxyl groups.

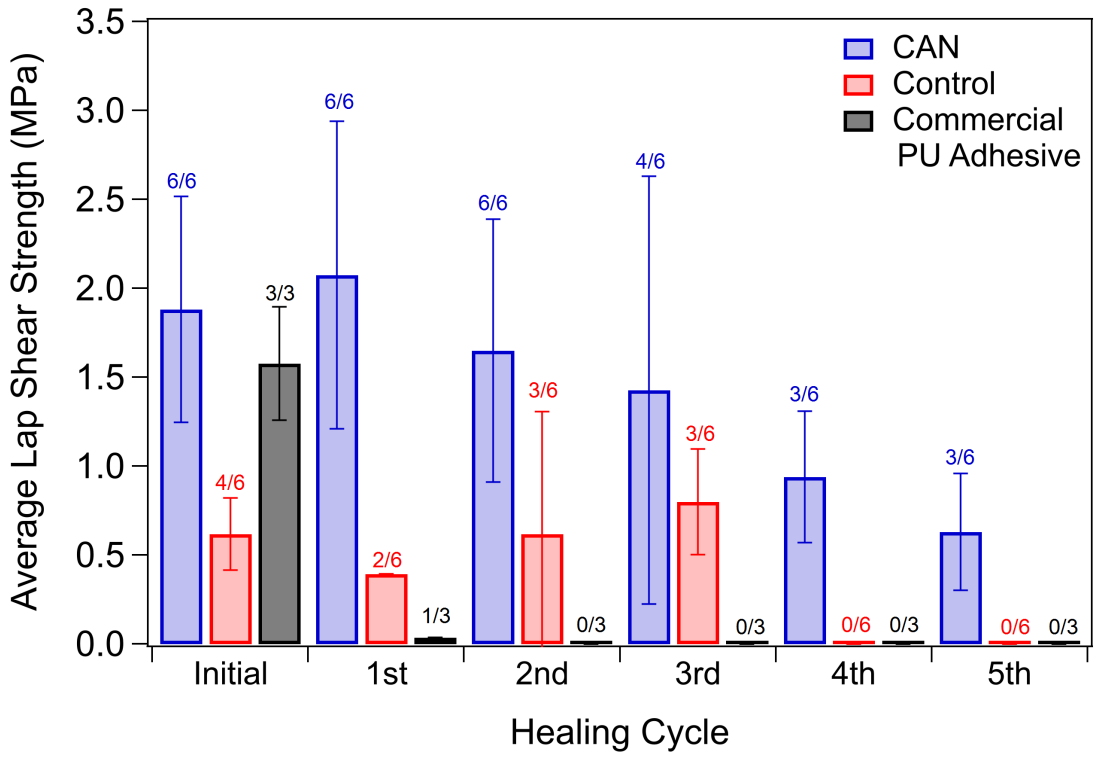

Figure 4. Lap shear strength of control film, CAN film, and commercial PU adhesive Gorilla Glue. Between each healing cycle, samples were clamped and cured at 150°C for 2 hours. The numbers above each bar indicate the number of measurable samples out of the total; other samples broke prior to testing.

While the CAN film is extremely strong, substrates can be recovered by simply heating the adhered sample, causing the covalent bonds to become dynamic and easily detach from the glass (Figure 5, Video S1). Additionally, the CAN film exhibited excellent water resistance. After submerging the prepared lap shear sample in DI water for 72 hours, the average lap shear strength remained constant (Figure S9). Directly converting the PU commercial adhesive to a CAN via the addition of carbamate exchange catalyst was limited by the blowing reaction between isocyanate and water. The exchange catalyst accelerated the blowing reaction, evidenced by obvious urea formation seen through excessive bubbling and a significant decrease in lap shear strength (Figure S10, Figure S11). These results demonstrate the versatility of dynamic networks, extending beyond

exchange within the network to transcarbamoylation between PU CAN films and surfaces for improved adhesive properties.

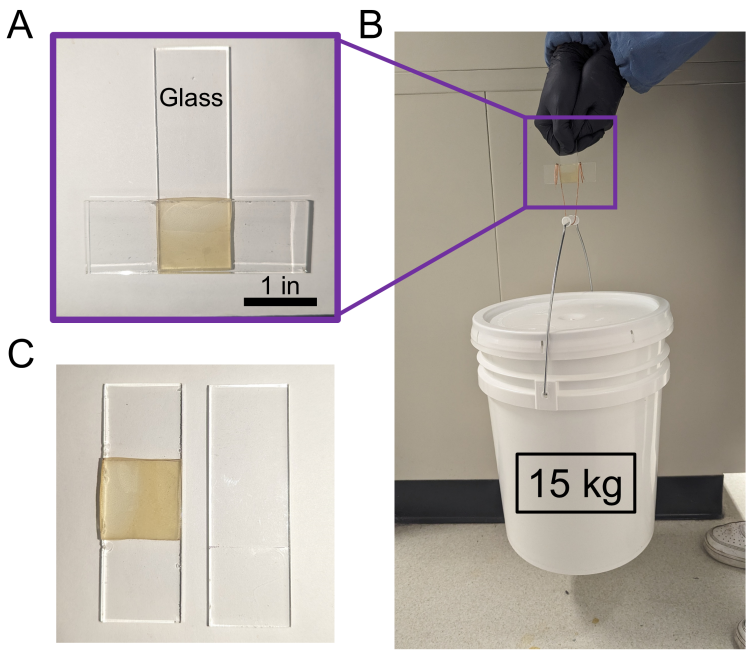

Figure 5. (A) Image of adhesive joint between two glass slides post curing for 2 hours at 150°C, CAN film area measuring 1 square inch. (B) CAN film adhered to glass can hold over 15 kg of weight without failure. (C) The sample was easily separated after heating with a heat gun for 30 seconds to recover substrates and adhesive film (Video S1).

The dynamic nature of the CAN film allowed for traditional thermoset material reprocessing using compression molding. To obtain a homogenous sample, the films were milled at cryogenic temperatures, producing a fine powder that was chemically identical to the pristine CAN film (Figure S12). This powder was compression molded at 150°C under 10 tons of ram force for 1 hour, resulting in homogenous films with near-identical chemical and network properties to the pristine CAN film, as determined by FT-IR and DMTA (Figure 6B, Figure S12, Figure S13, Table S1). Applying the same method to the control film did not produce a measurable sample (Figure 6C). Since the CAN film displayed a small beta transition in DMTA that was absent in the control film, slight differences in their mechanical properties are expected when measured

in the glassy state (Figure 2C, Figure 6A). When compared to the pristine CAN film, which had an average peak stress of 22 MPa and average peak strain of 148%, the reprocessed CAN film experienced slightly lower peak stress and peak strain of 18 MPa and 119% respectively (Figure 6A, Table 1). As a result, the Young's modulus slightly increases from 15.0 to 15.8 MPa after reprocessing, reflecting a slight increase in stiffness (Table 1). While these average values for the reprocessed film vary slightly from the pristine film, they agree within the uncertainty of each measurement (Table 1). Small deviations in mechanical properties are likely to arise due to changes of morphology or crosslinks in the random networks.[22, 37] Overall, the adhesive CAN films service life can be greatly extended by reprocessing and remolding material to fit application needs without sacrificing adhesive and mechanical properties.

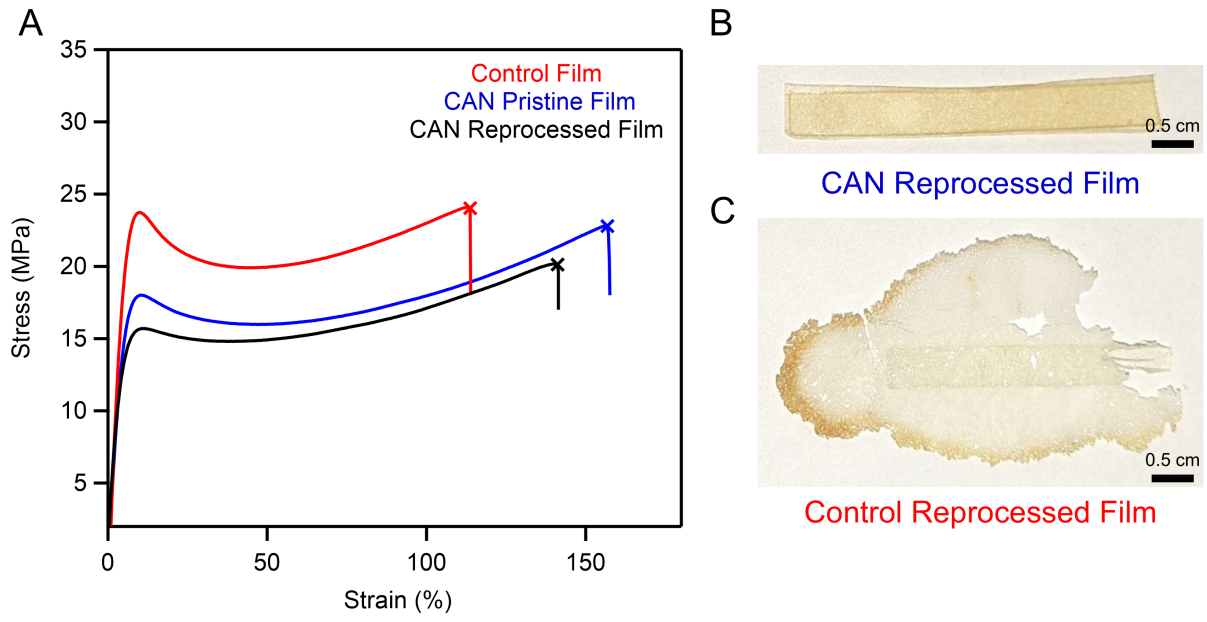

Figure 6. (A) Stress-strain curves for control film (red), pristine CAN film (blue), and reprocessed CAN film (black). (B) Image of reprocessed CAN film showing overall uniformity. (C) Image of reprocessed control film, from which a homogenous film was not obtained.

Sample	Average Peak Stress (MPa)	Average Peak Strain (%)	Average Young's Modulus (MPa)	Average Toughness (MPa)
Control	24.25 ± 1.10	112.80 ± 21.04	21.94 ± 3.12	2333 ± 464
CAN	22.11 ± 2.42	148.08 ± 23.25	15.03 ± 0.98	2632 ± 507
CAN Reprocessed	18.58 ± 1.12	118.86 ± 15.41	15.75 ± 1.13	1887 ± 280

Table 1. Mechanical properties of control film, pristine CAN film, and reprocessed CAN film.

Conclusions

In this work, we demonstrated the utility of PU CANs beyond reprocessability for the application of self-healing adhesives. Dynamic urethane bonds, facilitated by $Zr(tmhd)_4$, allowed the PU CAN to retain its adhesive strength over five healing cycles. Additionally, internal dynamic crosslinks in the CAN film permitted reprocessing using compression molding with no significant decrease in mechanical properties. Since PU CANs are highly tunable, this platform can be extended to a wide range of adhesive applications from construction to automotive to household environments.[3] Monomer structure can be varied for desired properties and curing a 2-part system directly on the adherends may impart additional strength. Moreover, many different substrates can be activated for use with PU CANs by exposing surface hydroxyl groups through simple means such as oxygen plasma etching. Since covalent bonding of the adhesive to the substrate is reversible, valuable parts such as composites may be recovered at the end of their lifetime by simply removing the adhesive using heat, allowing for reprocessing and reuse. This work helps to bring PU CANs closer to implementation at industrial scales to improve polymer economy circularity.

Experimental Methods

Materials. All reagents were purchased from Sigma-Aldrich or Fisher Scientific. Polyols were dried in a vacuum oven at 90 °C under 20 mTorr vacuum for 16 hours prior to film synthesis. All other reagents were used without further purification unless otherwise specified. Dichloromethane (DCM) and toluene were purchased from Sigma-Aldrich and dried using a custom-built solvent purification system (JC Myer System) with an alumina column. Borosilicate glass sheets (25.4 mm (W) x 3.175 mm (T) x 76.2 mm (L)) were purchased from McMaster-Carr and cleaned with acetone prior to use. Commercial polyurethane adhesive Gorilla Glue® (ASIN B01MDS317O) was purchased from Amazon.

Instrumentation. Infrared spectra were recorded on a ThermoFisher Nicolet iS20 with a ZnSe Smart iTR attachment. Spectra were uncorrected and normalized.

Dynamic mechanical thermal analysis (DMTA) was conducted on a TA Instruments RSA-G2 Solids Analyzer. Film samples were cut into rectangles (*ca.* 7 mm (W) x 1.5 mm (T) x 20 mm (L) and a gauge length of 10 mm) prior to analysis. The tension axial force was tared to 0 N and a strain adjustment was set to 30.0%, with a maximum strain of 10.0%, a minimum strain of 0.05%, maximum oscillation force of 0.01 N and maximum oscillation force of 0.2 N. A temperature sweep was conducted from -30°C to 150°C with a ramp rate of 5.0°C/min, with an oscillating strain of 0.05% and an angular frequency of 6.28 rad s^{-1} (1 Hz).

Stress relaxation analysis was performed on a TA Instruments RSA-G2 Solids Analyzer using rectangular films (*ca.* 7 mm (W) x 1.5 mm (T) x 20 mm (L) and a gauge length of 10 mm). A strain adjustment of 30.0% was set with a maximum strain of 10.0%, a minimum strain of 0.05%, maximum oscillation force of 0.01 N and maximum oscillation force of 0.2 N. The sample was equilibrated at 160 °C for 120 s, then a strain of 5.0% was applied. While applying the constant 5.0% strain, 6.0 points were sampled per second until the sample had completely relaxed stress (roughly 30 minutes). Reported values are expressed as averages with standard deviation of at least three replicates.

For reprocessing, samples were milled at cryogenic temperatures using a RETSCH CryoMill. Samples were milled for two cryogenic cycles with automatic cooling. After the system was cooled, approximately 6 minutes at a frequency of 5 Hz, the grinding time was set to 4 minutes at 30 Hz. This was repeated a second time, with an intermediate cooling time of 30 seconds at 5 Hz. The resulting polymer powder was then placed in a mold between two steel plates and pressed

using a preheated PHI 30-ton Manual Hydraulic Compression Press. Samples were compression molded for 1 hour at 150°C under 10 tons of pressure. The sample was removed from the mold either cut into rectangles or dog bone shaped tensile bars.

Tensile testing was performed using an MTS Criterion Universal Test System with a 2.5 kN load cell following ASTM D-1708. Film samples were cut into dog bone shaped bars (*ca.* 5 mm (W) x 2 mm (T) x 25 mm (L) and a gauge length of 16 mm) using a die-press. Samples were pulled at a uniaxial extension rate of 0.5 mm/s at ambient temperature. Young's Modulus was calculated from the peak stress and peak strain. Toughness was calculated by integrating the stress strain curve. All values are reported as averages and standard deviation of at least five replicates.

Differential Scanning Calorimeter under a nitrogen atmosphere. Samples (5-10 mg) were heated to 120.00 °C at a rate of 10.00 °C/min to erase thermal history. The samples were then cooled to -30.00 °C at 10.00 °C/min, then heated to 150.00 °C. Displayed differential thermograms are from the second heating ramp. The glass transition temperature (T_g) was calculated from the maximum value of the derivative of heat flow with respect to temperature.

Lap shear testing was performed using a MTS Criterion Universal Test System with a 2.5 kN load cell following ASTM D-1002-10. Samples were cut into rectangles (*ca.* 25.4 mm (W) x 1.5 mm (T) x 12.7 mm (L)) using shears and borosilicate glass substrates (25.4 mm (W) x 3.175 mm (T) x 76.2 mm (L) unless otherwise noted) were cleaned with acetone. Metal binder clips were used to clamp samples between two glass substrates with a joint overlap area of 25.4 mm (W) x 12.7 mm (L). Spacers identical to the thickness of the sample film were used to ensure substrate alignment. Samples were cured at 150°C for two hours. To prepare the commercial PU adhesive lap shear samples, glass substrates were first cleaned with acetone, then the joint overlap area was wetted with water. A thin layer of Gorilla Glue® was spread in the overlap area and the substrates were clamped together and cured at room temperature for 24 hours. Lap shear testing was conducted using offset grips and samples were pulled at a rate of 0.05 in/min with a data acquisition rate of 5.0 Hz. Average lap shear strength was calculated using the load at failure and adhesive joint area. Average lap shear strength values represent the average of at least three replicates, including samples with a lap shear strength of zero, which broke prior to measurement. Error bars represent the standard deviation of the measurable samples. The samples tested in Figure S1 and Figure S10 were not measured in triplicate, values are reported for a single measurement. After

initial lap shear testing, all free substrates were cleaned with acetone. The lap shear samples were then healed by clamping together with metal binder clips and appropriate spacers and cured for 2 hours at 150 °C. This process was repeated for five healing cycles. Statistical analysis was performed using a one-tailed T-test with unequal variance to determine significance levels. The recovery ratio was calculated based on the average lap shear strength with respect to the previous cycle's average lap shear strength. The recovery ratios for all healing cycles were then averaged. For silanization, the glass substrates were soaked in a solution of 5% (v/v%) of dichlorodimethylsilane in dry toluene for 30 minutes. The substrates were rinsed three times with dry toluene, then rinsed three times with dry methanol, and dried overnight at 150°C prior to lap shear sample preparation as described above. A set of glass substrates was cleaned under O_2 plasma (Harrick Plasma) for 5 minutes at 10.5 W radiofrequency power with a pressure of around 200 mTorr, then lap shear samples were prepared as described above.

Thermogravimetric analysis (TGA) was performed on a TA Instruments TGA5500 using 15-20 mg of sample. Samples were heated under nitrogen atmosphere at a rate of 10.00 °C/min from 25 °C to 500 °C. For isothermal TGA, samples were heated under air and held at 150 °C for 16 hours. Buoyancy effect for air was corrected by measuring the empty crucible under the same measurement conditions used for the samples. Performance of the thermobalance of the STA was verified by using a certified sample of calcium oxalate monohydrate (European Pharmacopoeia Reference Standard) up to 1000 °C.

Synthesis of Crosslinked Polyurethane Adhesive CAN Films: Polyol components were dried under 20 mTorr vacuum at 90 °C for 16 hours prior to use. In a 40 mL scintillation vial, poly[trimethylolpropane/di(propylene glycol)-alt-adipic acid/phthalic anhydride], polyol (-OH equivalent 2.5, 1.00 g, 2.00 mmol), polypropylene glycol (1000 g/mol, 3.83 g, 3.83 mmol), pentaerythritol propoxylate (5/4 PO/OH, 426 g/mol, 1.50 g, 3.52 mmol), and zirconium tetrakis(2,2,6,6-tetramethyl-3,5-heptanedionate) (0.23 g, 0.28 mmol, 1 mol% wrt urethane) were dissolved in dry DCM by vortexing. To this solution, 4,4′-methylenebis(phenyl isocyanate) (3.45 g, 13.78 mmol) was added and sonicated and vortexed until complete dissolution. The solution was cast into an aluminum pan and cured at room temperature for 24 hours, then post-cured for 48 hours in a vacuum oven under 20 mTorr vacuum at 90 °C.

CAN Film:

FT-IR (solid, ATR) 3303 (N-H stretch), 2967 (sp^3 C-H stretch), 2866 (sp^3 C-H stretch), 1725 (C=O stretch), 1709 (C=O stretch), 1596, 1530 (N-H deformation), 1511 (N-H deformation), 1453, 1412, 1375, 1308, 1221, 1069 (C-N stretch), 1017, 930, 815, 767, 607 cm^{-1}.

Synthesis of Crosslinked Polyurethane Adhesive Control Films: Polyol components were dried under 20 mTorr vacuum at 90 °C for 16 hours prior to use. In a 40 mL scintillation vial, poly[trimethylolpropane/di(propylene glycol)-alt-adipic acid/phthalic anhydride], polyol (-OH equivalent 2.5, 1.00 g, 2.00 mmol), polypropylene glycol (1000 g/mol, 4.01 g, 4.01 mmol), and pentaerythritol propoxylate (5/4 PO/OH, 426 g/mol, 1.50 g, 3.52 mmol) were dissolved in dry toluene by vortexing. To this solution, 4,4′-methylenebis(phenyl isocyanate) (3.50 g, 13.96 mmol) was added The solution was heated at 60 °C and vortexed until completely dissolved. The solution was then cast into an aluminum pan and cured at 60 °C for 18 hours, then 100 °C for 4 hours, then 140 °C for 2 hours, then post-cured for 16 hours in a vacuum oven under 20 mTorr vacuum at 90 °C.

Control Film:

FT-IR (solid, ATR) 3304 (N-H stretch), 2969 (sp^3 C-H stretch), 2917 (sp^3 C-H stretch), 2870 (sp^3 C-H stretch), 1725 (C=O stretch), 1709 (C=O stretch), 1597, 1533 (N-H deformation), 1513 (N-H deformation), 1453, 1412, 1374, 1309, 1222, 1069 (C-N stretch), 1017, 928, 815, 768, 706, 611 cm^{-1}.

ASSOCIATED CONTENT

Supporting Information

Lap shear, DSC plots, SRA plots, relaxation spectra, TGA plots, FT-IR spectra, DMTA plots, (Figures S1-S13), equations (Equations S1-S3), and data tables (Tables S1-S3). (PDF)

Video S1 (mp4) Separation of the prepared CAN sample upon heating using a heat gun.

AUTHOR INFORMATION

Corresponding Authors

WRD: wdichtel@northwestern.edu

Acknowledgement

The authors thank Janan Hui for assistance in plasma treating substrates. The authors also thank Dr. Carla Shute for her contributions to lap shear testing and her expertise in instrument troubleshooting. This research was supported by the National Science Foundation (NSF) through the Center for Sustainable Polymers (CHE-1901635) and the U.S. Department of Energy's Office of Energy Efficiency and Renewable Energy (EERE) under the Advanced Manufacturing Office Award Number DE-EE0007897 awarded to the REMADE Institute, a division of Sustainable Manufacturing Innovation Alliance Corp. This work made use of the CLaMMP Facility and MatCI Facility which has received support from the MRSEC Program (NSF DMR-1720139) of the Materials Research Center at Northwestern University, the Center for Hierarchical Materials Design and from Northwestern University. This work made use of the IMSERC Physical Characterization facility at Northwestern University, which has received support from the Soft and Hybrid Nanotechnology Experimental (SHyNE) Resource (NSF ECCS-2025633), and Northwestern University.

Conflict of Interest Disclosure:

Northwestern University has filed a provisional patent application related to the findings described in this manuscript.

References

(1) *Structural Adhesives Chemistry and Technology*; Springer, 2012. DOI: 10.1007/978-1-4684-7781-8.

(2) Burchardt, B. 3 - Advances in polyurethane structural adhesives. In *Advances in Structural Adhesive Bonding*, Dillard, D. A. Ed.; Woodhead Publishing, 2010; pp 35-65.

(3) A. Pizzi., K. L. M. *Handbook of Adhesive Technology*; 2003.

(4) Bishopp, J. A.; Davies, L.; Haslam, J. J. Chemical and mechanical characterization of adhesive matrices. *Int. J. Adhes. Adhes.* **1993**, *13* (2), 111-119. DOI: 10.1016/0143-7496(93)90022-2.

(5) Osman, M. A.; Mittal, V.; Morbidelli, M.; Suter, U. W. Polyurethane Adhesive Nanocomposites as Gas Permeation Barrier. *Macromolecules* **2003**, *36* (26), 9851-9858. DOI: 10.1021/ma035077x.

(6) Li, Z.; Zhang, R.; Moon, K.-S.; Liu, Y.; Hansen, K.; Le, T.; Wong, C. P. Highly Conductive, Flexible, Polyurethane-Based Adhesives for Flexible and Printed Electronics. *Adv. Funct. Mater.* **2013**, *23* (11), 1459-1465. DOI: 10.1002/adfm.201202249.

(7) Leitsch, E. K.; Heath, W. H.; Torkelson, J. M. Polyurethane/polyhydroxyurethane hybrid polymers and their applications as adhesive bonding agents. *Int. J. Adhes. Adhes.* **2016**, *64*, 1-8. DOI: 10.1016/j.ijadhadh.2015.09.001.

(8) Faneco, T. M. S.; Campilho, R. D. S. G.; Silva, F. J. G.; Lopes, R. M. Strength and Fracture Characterization of a Novel Polyurethane Adhesive for the Automotive Industry. *J. Test. Eval.* **2017**, *45* (2), 398-407. DOI: 10.1520/JTE20150335.

(9) Yang, Y.; Du, F.-S.; Li, Z.-C. Highly Stretchable, Self-Healable, and Adhesive Polyurethane Elastomers Based on Boronic Ester Bonds. *ACS Appl. Polym. Mater.* **2020**, *2* (12), 5630-5640. DOI: 10.1021/acsapm.0c00941.

(10) Szycher, M. Szycher's Handbook of Polyurethanes. *J. Am. Chem. Soc.* **2000**, *122* (16), 3983-3983. DOI: 10.1021/ja004704k.

(11) Wang, S.; Liu, Z.; Zhang, L.; Guo, Y.; Song, J.; Lou, J.; Guan, Q.; He, C.; You, Z. Strong, detachable, and self-healing dynamic crosslinked hot melt polyurethane adhesive. *Mater. Chem. Front.* **2019**, *3* (9), 1833-1839. DOI: 10.1039/C9QM00233B.

(12) Bowman, C.; Du Prez, F.; Kalow, J. Introduction to chemistry for covalent adaptable networks. *Polym. Chem.* **2020**, *11* (33), 5295-5296. DOI: 10.1039/D0PY90102D.

(13) Zhang, Y.; Zhang, L.; Yang, G.; Yao, Y.; Wei, X.; Pan, T.; Wu, J.; Tian, M.; Yin, P. Recent advances in recyclable thermosets and thermoset composites based on covalent adaptable networks. *J. Mater. Sci. Technol.* **2021**, *92*, 75-87. DOI: 10.1016/j.jmst.2021.03.043.

(14) Kloxin, C. J.; Bowman, C. N. Covalent adaptable networks: smart, reconfigurable and responsive network systems. *Chem. Soc. Rev.* **2013**, *42* (17), 7161-7173. DOI: 10.1039/C3CS60046G.

(15) Cui, C.; Chen, X.; Ma, L.; Zhong, Q.; Li, Z.; Mariappan, A.; Zhang, Q.; Cheng, Y.; He, G.; Chen, X.; et al. Polythiourethane Covalent Adaptable Networks for Strong and Reworkable Adhesives and Fully Recyclable Carbon Fiber-Reinforced Composites. *ACS Appl. Mater. Interfaces* **2020**, *12* (42), 47975-47983. DOI: 10.1021/acsami.0c14189.

(16) Li, L.; Chen, X.; Torkelson, J. M. Covalent Adaptive Networks for Enhanced Adhesion: Exploiting Disulfide Dynamic Chemistry and Annealing during Application. *ACS Appl. Polym. Mater.* **2020**, *2* (11), 4658-4665. DOI: 10.1021/acsapm.0c00720.

(17) Yang, S.; Bai, J.; Sun, X.; Zhang, J. Robust and healable poly(disulfides) supramolecular adhesives enabled by dynamic covalent adaptable networks and noncovalent hydrogen-bonding interactions. *Chem. Eng. J.* **2023**, *461*, 142066. DOI: 10.1016/j.cej.2023.142066.

(18) Rahman, M. A.; Bowland, C.; Ge, S.; Acharya, S. R.; Kim, S.; Cooper, V. R.; Chen, X. C.; Irle, S.; Sokolov, A. P.; Savara, A.; et al. Design of tough adhesive from commodity thermoplastics through dynamic crosslinking. *Sci. Adv.* **2021**, *7* (42), eabk2451. DOI: 10.1126/sciadv.abk2451.

(19) Yan, Q.; Zhou, M.; Fu, H. A reversible and highly conductive adhesive: towards self-healing and recyclable flexible electronics. *J. Mater. Chem. C* **2020**, *8* (23), 7772-7785. DOI: 10.1039/C9TC06765E.

(20) Chazovachii, P. T.; Somers, M. J.; Robo, M. T.; Collias, D. I.; James, M. I.; Marsh, E. N. G.; Zimmerman, P. M.; Alfaro, J. F.; McNeil, A. J. Giving superabsorbent polymers a second life as pressure-sensitive adhesives. *Nat. Commun.* **2021**, *12* (1), 4524. DOI: 10.1038/s41467-021-24488-9.

(21) Zhao, X.-L.; Li, Y.-D.; Weng, Y.; Zeng, J.-B. Biobased epoxy covalent adaptable networks for high-performance recoverable adhesives. *Ind. Crops. Prod.* **2023**, *192*, 116016. DOI: 10.1016/j.indcrop.2022.116016.

(22) Putnam-Neeb, A. A.; Stafford, A.; Babu, S.; Chapman, S. J.; Hemmingsen, C. M.; Islam, M. S.; Roy, A. K.; Kalow, J. A.; Varshney, V.; Nepal, D.; et al. Oligosiloxane-Based Epoxy Vitrimers: Adaptable Thermosetting Networks with Dual Dynamic Bonds. *ACS Appl. Polym. Mater.* **2024**. DOI: 10.1021/acsapm.3c03082.

(23) Montarnal, D.; Capelot, M.; Tournilhac, F.; Leibler, L. Silica-Like Malleable Materials from Permanent Organic Networks. *Science* **2011**, *334* (6058), 965-968. DOI: 10.1126/science.1212648.

(24) Yue, L.; Guo, H.; Kennedy, A.; Patel, A.; Gong, X.; Ju, T.; Gray, T.; Manas-Zloczower, I. Vitrimerization: Converting Thermoset Polymers into Vitrimers. *ACS Macro Lett.* **2020**, *9* (6), 836-842. DOI: 10.1021/acsmacrolett.0c00299.

(25) Li, X.; Qiu, X.; Yang, X.; Zhou, P.; Guo, Q.; Zhang, X. Multi-Modal Melt-Processing of Birefringent Cellulosic Materials for Eco-Friendly Anti-Counterfeiting. *Adv. Mater.* **2024**, *n/a* (n/a), 2407170. DOI: 10.1002/adma.202407170.

(26) Liang, C.; Gracida-Alvarez, U. R.; Gallant, E. T.; Gillis, P. A.; Marques, Y. A.; Abramo, G. P.; Hawkins, T. R.; Dunn, J. B. Material Flows of Polyurethane in the United States. *Environ. Sci. Technol.* **2021**, *55* (20), 14215-14224. DOI: 10.1021/acs.est.1c03654.

(27) OECD. *Global Plastics Outlook*; 2022. https://www.oecd-ilibrary.org/content/publication/aa1edf33-en DOI: 10.1787/aa1edf33-en.

(28) Sheppard, D. T.; Jin, K.; Hamachi, L. S.; Dean, W.; Fortman, D. J.; Ellison, C. J.; Dichtel, W. R. Reprocessing Postconsumer Polyurethane Foam Using Carbamate Exchange Catalysis and Twin-Screw Extrusion. *ACS Cent. Sci.* **2020**, *6* (6), 921-927. DOI: 10.1021/acscentsci.0c00083.

(29) Fortman, D. J.; Sheppard, D. T.; Dichtel, W. R. Reprocessing Cross-Linked Polyurethanes by Catalyzing Carbamate Exchange. *Macromolecules* **2019**, *52* (16), 6330-6335. DOI: 10.1021/acs.macromol.9b01134.

(30) Swartz, J. L.; Elling, B. R.; Castano, I.; Thompson, M. P.; Sheppard, D. T.; Gianneschi, N. C.; Dichtel, W. R. Copolymers Prepared by Exchange Reactions Enhance the Properties of Miscible Polymer Blends. *Macromolecules* **2022**, *55* (19), 8548-8555. DOI: 10.1021/acs.macromol.2c01268.

(31) Ferraz da Silva, I.; Freitas-Lima, L. C.; Graceli, J. B.; Rodrigues, L. C. M. Organotins in Neuronal Damage, Brain Function, and Behavior: A Short Review. (1664-2392 (Print)). DOI: 10.3389/fendo.2017.00366 From 2017.

(32) Sun, M.; Sheppard, D. T.; Brutman, J. P.; Alsbaiee, A.; Dichtel, W. R. Green Catalysts for Reprocessing Thermoset Polyurethanes. *Macromolecules* **2023**, *56* (17), 6978-6987. DOI: 10.1021/acs.macromol.3c01116.

(33) Kim, S.; Swartz, J. L.; Sala, O.; Sun, M.; Oanta, A. K.; Brutman, J. P.; Alsbaiee, A.; Dichtel, W. R. Thermal Activation of Zirconium(IV) Acetylacetonate Catalysts to Enhance Polyurethane Synthesis and Reprocessing. *Macromolecules* **2024**, *57* (14), 6759-6768. DOI: 10.1021/acs.macromol.4c00625.

(34) Chen, Z.; Sun, Y.-C.; Wang, J.; Qi, H. J.; Wang, T.; Naguib, H. E. Flexible, Reconfigurable, and Self-Healing TPU/Vitrimer Polymer Blend with Copolymerization Triggered by Bond Exchange Reaction. *ACS Appl. Mater. Interfaces* **2020**, *12* (7), 8740-8750. DOI: 10.1021/acsami.9b21411.

(35) Farzaneh, S.; Fitoussi, J.; Lucas, A.; Bocquet, M.; Tcharkhtchi, A. Shape memory effect and properties memory effect of polyurethane. *J. Appl. Polym. Sci.* **2013**, *128* (5), 3240-3249. DOI: 10.1002/app.38530.

(36) Delebecq, E.; Pascault, J.-P.; Boutevin, B.; Ganachaud, F. On the Versatility of Urethane/Urea Bonds: Reversibility, Blocked Isocyanate, and Non-isocyanate Polyurethane. *Chem. Rev.* **2013**, *113* (1), 80-118. DOI: 10.1021/cr300195n.

(37) Peterson, G. I.; Ko, W.; Hwang, Y.-J.; Choi, T.-L. Mechanochemical Degradation of Amorphous Polymers with Ball-Mill Grinding: Influence of the Glass Transition Temperature. *Macromolecules* **2020**, *53* (18), 7795-7802. DOI: 10.1021/acs.macromol.0c01510.

TOC IMAGE

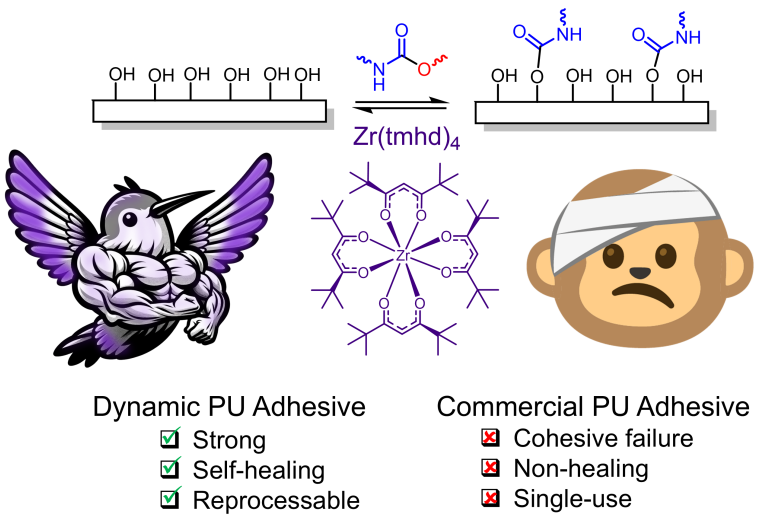
OH OH OH OH OH OH
Zr(tmhd)4
Dynamic PU Adhesive
Strong
Self-healing
Reprocessable
Commercial PU Adhesive
Cohesive failure
Non-healing
Single-use